

Nonlinear analysis of magnetospheric data Part II. Dynamical characteristics of the AE index time series and comparison with nonlinear surrogate data

G. P. Pavlos¹, D. Kugiuntzis², M. A. Athanasiu¹, N. Hatzigeorgiu³, D. Diamantidis¹, and E. T. Sarris¹

¹Department of Electrical and Computer Engineering, Demokritos University of Thrace, 67100 Xanthi, Greece

²Max-Planck Institute for Physics of Complex Systems, 01187 Dresden, Germany

³Institute for Language and Speech Processing, Xanthi Branch, Greece

Received: 09 January 1999 – Accepted: 17 April 1999

Abstract. In this study we have used dynamical characteristics such as Lyapunov exponents, nonlinear dynamic models and mutual information for the nonlinear analysis of the magnetospheric AE index time series. Similarly with the geometrical characteristic studied in Pavlos et al. (1999b), we have found significant differences between the original time series and its surrogate data. These results also suggest the rejection of the null hypothesis that the AE index belongs to the family of stochastic linear signals undergoing a static nonlinear distortion. Finally, we believe that these results support the hypothesis of nonlinearity and chaos for the magnetospheric dynamics.

1 Introduction

In recent years many nonlinear models of magnetospheric dynamics were developed, which could bear low-dimensional chaotic solutions (Baker et al., 1990; Klimas et al., 1991; Pavlos et al., 1994). These results were in agreement with chaotic analysis of magnetospheric experimental time series (Vassiliadis et al., 1990, 1992; Robert et al., 1991; Shan et al., 1991; Pavlos et al., 1992a,b, 1994). A series of significant studies (Price and Prichard, 1993; Price et al., 1994; Prichard, 1994) showed the weakness of the nonlinear analysis of the magnetospheric time series especially in relation with the strong null hypothesis for stochasticity of Theiler (Theiler et al., 1992a,b). For a review of studies of the nonlinear dynamics of the magnetosphere refer to Klimas et al. (1996).

In a study by Pavlos et al. (1999b), which is described as Part I we have used correlation dimension and other geometrical quantities estimated for the AE index time series, observed in the last six months of the year 1978, as discriminating statistics between nonlinear dynamics and linear stochastic signals. The AE index describes the Auroral-zone magnetic activity which is related with the global magnetospheric dynamics through a complex system of currents. The

null hypothesis which tested concerns the observed time series that arises by a static non linear distortion of a Gaussian signal $x(t) = h(s(t))$, where h is a monotonic nonlinear function. (Theiler et al., 1992b,a; Schreiber and Schmitz, 1996; Schreiber, 1998). The discriminating statistics of the geometrical characteristics showed strong inconsistency of the AE index time series to the null hypothesis of Gaussian linear stochastic signal which share the same power spectrum and amplitude distribution with the observed time series. We must point out here that the geometric characteristics are measures of the spatial distribution of the sample of points along a system orbit in the reconstructed phase space of the system. In this case there is no information about the dynamic evolution of the system in the phase space. Dynamic characteristics that connect current and future states of the system are the Lyapunov exponents, the average mutual information and predictors (local or global). In this work we use dynamical characteristics as discriminating statistics on the AE index time series. Prediction methods have already been used for the nonlinear analysis of the response to the solar wind of the magnetosphere as given by the AE index observed during short periods (Price and Prichard, 1993; Price et al., 1994). The input/output prediction methods used by the authors of these papers showed in some cases evidence for non-linear response of the earth's magnetosphere while in other cases little or no evidence for nonlinear coupling was found. Before these studies, it has been suggested that the solar wind-magnetosphere interaction is a dynamic non linear phenomenon, by using linear prediction filter techniques. These techniques have shown two distinct physical mechanisms for the magnetospheric response to solar wind. The first mechanism corresponds to a directly driven process and the second to a storage-release mechanism (Bargatze et al., 1985; McPerron et al., 1988; Klimas et al., 1996, 1997). The second mechanism could be thought as related to a chaotic process in accordance with the above referred nonlinear magnetospheric modeling. In order to test this hypothesis we study here dynamical characteristics as discriminating statistics between the magnetospheric AE index

and stochastic signals (surrogate data). Our statistical analysis uses the dynamical characteristics: Lyapunov exponents, mutual information and models for prediction showed significant inconsistency between the AE index process and the null hypothesis of an underlying Gaussian linear stochastic process. Our results strengthen the hypothesis of magnetospheric chaos especially in relation to the second storage-release mechanism.

In Sect. 2, we present the theoretical framework of our study which is related to the dynamical characteristics of the AE index time series. Section 3 includes the results of the comparison between the AE index and its surrogates on the dynamical characteristics, i.e. spectrum of Lyapunov exponents, local linear prediction, global linear and nonlinear polynomial fitting, and mutual information. Section 4 includes the summary and the discussion about these results.

2 Theoretical framework

In order to emphasize the significance and the physical meaning of the nonlinear analysis of an experimental time series, we must look for the type of the dynamical system that is likely to generate the observed time series (e.g. deterministic or stochastic, linear or nonlinear, externally driven or not). When a significant external stochastic input (white or colored) is supposed, then the underlying system is regarded as stochastic. Of course a stochastic component can also be caused by internal microscopic processes of the system, which is possible for the magnetospheric data we study here.

Non linear analysis of experimental time series concerning geometrical and dynamical characteristics can give significant information about the deterministic component of the underlying process. Assuming the stochastic component is small, the deterministic part of the underlying dynamics of a real time series is most probably assigned to a nonlinear dissipative system. A nonlinear dissipative system can reveal rich dynamics and its solution in phase space can be a periodic orbit (limit cycle), a quasi-periodic orbit (torus) or a non-periodic orbit forming a strange attractor in phase space. A strange attractor of a fractal non-integer dimension corresponds to a contracting flow $\mathbf{f}^t(\mathbf{s}_0)$ (for an initial d -dimensional state vector \mathbf{s}_0) with sensitive dependence to the initial conditions (e.g. see Eckmann and Ruelle (1985), Tsonis (1992), Isham (1993)). As stochastic systems can also give non-periodic solutions, it is crucial to investigate whether an observed time series corresponds to a stochastic system or to a nonlinear deterministic system with chaotic (strange) attractor solution.

According to the embedding theory reviewed in Part I (Pavlos et al., 1999a), the dynamics of the underlying process of an experimental time series $\mathbf{x}(i) = \mathbf{x}(t_i)$ can be equivalently represented in the reconstructed phase space R^m , simply as $\mathbf{x}(i) = [x(i), x(i-\tau), \dots, x(i-(m-1)\tau)]^T$ for $m \geq 2d+1$ and τ a delay parameter (Takens, 1981). The mirrored dynamics in the reconstructed phase space is

$$\mathbf{x}(i+1) = \mathbf{F}(\mathbf{x}(i)) \quad (1)$$

or assuming only the first component of $\mathbf{x}(i+1)$

$$x(i+1) = F(x(i), x(i-\tau), x(i-(m-1)\tau)) \quad (2)$$

where F is the scalar function being the first component of the vector function \mathbf{F} . For systems involving a significant stochastic component, Eqs. (1) and (2) have to be modified to account for the observational or dynamical noise. Generally, when an infinite dimensional stochastic signal acts as an input to a low dimensional dynamics then it is possible to extract with sufficient confidence conclusions about the underlying dynamics (Argyris et al., 1998a,b; Pavlos et al., 1999b).

In this study we estimate the dynamical characteristics of the reconstructed dynamics (\mathbf{F} or F) and reflect the results back to the original magnetospheric dynamics underlying to the observed AE index time series. Particularly, we aim at understanding the nature of \mathbf{F} that corresponds to the magnetospheric dynamics.

A linear stochastic system can mimic low dimensional chaos. To exclude this possibility we test the general null hypothesis that the observed signal arises from a linear stochastic process undergoing static distortion following the surrogate data test (Theiler et al., 1992a,b). In part I, we did this for the geometrical characteristics. Here, we focus on dynamical characteristics and use prediction, Lyapunov spectrum and mutual information as the discriminating statistics between the surrogate data and the original time series.

2.1 The spectrum of the Lyapunov exponents

The spectrum of Lyapunov exponents measures the rate of convergence or divergence of close trajectories in all d directions of the phase space. A positive Lyapunov exponent regards divergence of trajectories in one direction, or alternatively expansion of an initial volume in this direction, and a negative Lyapunov exponent regards convergence of trajectories or contraction of volume along another direction. For flows, there is always a zero Lyapunov exponent for the direction of the flow. The Lyapunov exponents are thus ordered as $\lambda_1 \geq \dots \geq \lambda_d$ and a positive λ_1 indicates chaos for a dissipative deterministic system.

The spectrum of the Lyapunov exponents can be estimated from a time series by following the evolution of small perturbations of the reconstructed orbit making use of the linearized reconstructed dynamics. The evolution of the displacement vector between the neighboring points $\mathbf{x}(i)$ and $\mathbf{y}(i) + \mathbf{w}(i)$ in the reconstructed phase space is given by the equation

$$\mathbf{w}(i+1) = \mathbf{DF}(\mathbf{x}(i))\mathbf{w}(i) \quad (3)$$

where \mathbf{DF} is the derivative matrix of \mathbf{F} (see Eq. 1). A local approximation of the matrix \mathbf{DF} can be found by solving the minimization problem

$$\min_{A_i} S = \min_{A_i} \frac{1}{k} \sum_{j=1}^k \|\mathbf{w}_j(i+1) - A_i \mathbf{w}_j(i)\| \quad (4)$$

where k is the number of the neighbors to $\mathbf{x}(i)$ regarding k different perturbations \mathbf{w}_j , $j = 1, \dots, k$, which are used to estimate $\mathbf{A}_i \equiv \mathbf{DF}$ at the point $\mathbf{x}(i)$.

The Lyapunov spectrum is found by repeating this process for all N reconstructed points $\mathbf{x}(i)$, $i = 1, \dots, N$, as

$$\lambda_j = \sum_{i=1}^N \log(\|\mathbf{A}_i \mathbf{e}_j^i\|) \quad (5)$$

where a new set of orthogonal vectors $\{\mathbf{e}_j^i\}$ is produced by reorthonormalization of the vectors at time i $\{\mathbf{A}_{i-1} \mathbf{e}_j^{i-1}\}$ in order to retain the local orthogonal spanning of the state space (Sano and Sawada, 1985; Eckman et al., 1986; Holz- fuss and Lauterborn, 1989; Karadonis and Pagitsas, 1995).

For the estimation of the maximum Lyapunov exponent (L_{max}) we use the equation

$$L_{max} = \lim_{\substack{t \rightarrow \infty \\ d(0) \rightarrow 0}} \frac{1}{t} \ln \left[\frac{d(t)}{d(0)} \right] \quad (6)$$

where $d(t) = |\mathbf{x}_2(t) - \mathbf{x}_1(t)|$ measures the separation between neighboring points in the reconstructed phase space (Wolf et al., 1985). Certainly, for finite data the initial $d(0)$ is limited by the distance of the closest neighbors and the time t is limited to the time period of the observation.

2.2 Modeling and prediction

The observable information $\mathbf{x}(t_i) = \mathbf{x}(i)$ on the temporal evolution of the orbit in the reconstructed phase space can be used for prediction or modeling purposes building the map $\mathbf{F}(\mathbf{x}(i))$ or $F(\mathbf{x}(i))$ (see Eqs. 1 and 2, respectively, here we proceed with F). Experimental estimation of the map F , and for T time steps ahead F^T , reduces to determining a group of parameters \mathbf{a} given a class of functional forms for $F^T(\mathbf{x}(i), \mathbf{a})$. For a given functional form of F^T we choose the parameters \mathbf{a} by using some form of cost function which measures the equality of matching the observed future sample $x(i+T)$ with the predicted $\hat{x}(i+T) = F^T(\mathbf{x}(i), \mathbf{a})$ (see Abarbanel et al. (1993)).

In this study we construct both linear and nonlinear maps as well as local or global looking for the best approximation to F^T . Modeling and prediction makes use of phase space reconstruction, implicitly (like the autoregressive (AR) models) or explicitly (like the local linear maps) (Weigend and Gershenfeld, 1993). Also the map $F^T(\mathbf{x}(i), \mathbf{a})$ may be approximated with different functional forms of global, local or semi-local type (Lillekjendlie et al., 1994). For any functional form, the parameters involved are estimated directly from the data. For modeling we make use of the whole set of the available data to fit the model, while for prediction we use a subset to fit the model (training set) and the rest to test the predictability of the estimated model (test set).

To verify the performance of the model, two measures of the modeling or prediction error are often computed. The first, is the normalized root mean square error (NRMSE), which is the root of the mean square differences of the modeled (or predicted) values from the actual values, normalized

with the standard deviation of the data. If $\text{NRMSE} \cong 0$ perfect model performance is achieved and if $\text{NRMSE} > 1$ the modeling or prediction is worse than this obtained using the mean value as model. The other measure is the correlation coefficient (CC), which estimates the correlation between the modeled (or predicted) data and the actual data and is obtained from the ratio of their covariance over the root of product of their variance alone. Note that CC takes values in $[-1, 1]$. When $\text{CC} \cong 1$ best correlations are obtained, i.e. the performance of the model is excellent, while for small CC-values close to zero or negative the performance is very poor.

In this work, F^T is approximated with global polynomials (linear and nonlinear) and local linear models.

2.2.1 Global polynomials

A simple approximation of F^T is with a single polynomial, which may involve only linear terms (this is actually the autoregressive (AR) model) or nonlinear terms as well of a degree q . Certainly, a polynomial of a small degree q in m delay variables, call it p_q^T , cannot model complicated dynamics and for pure chaotic systems is more likely to be insufficient. However, dealing with real data, this may turn out to be more an advantage, modeling only the evident dynamics (linear or nonlinear) and leaving the profound deterministic elements unmodeled, which as well may be masked by noise.

The general form of p_q^T where, $\hat{x}_{i+T} = p_q^T(\mathbf{x}_i)$, $\mathbf{x}_i \in R^m$ is given by the Volterra Wiener series of degree q and memory m

$$\begin{aligned} \hat{x}(i+T) = & a_0 + a_1 x(i) + a_2 x(i-\tau) \\ & + \dots + a_m x(i-(m-1)\tau) + \dots \\ & + a_{m+1} x^2(i) + a_m + 2x(i)x(i-\tau) \\ & + \dots + a_M x^q(i-(M-1)\tau)^q \end{aligned} \quad (7)$$

where $M = \frac{(m+q)!}{(m!q!)}$. In our work we use $q = 2$ because we are interested only to investigate the existence of nonlinearity in the data. Moreover, we construct all M polynomials starting with the constant term and adding one term of the Volterra series at a time.

2.2.2 Local Models

The idea with local models is that for deterministic systems, nearby trajectories evolve similarly, at least for a short time if the system is chaotic. Thus on the reconstructed attractor, for any point $\mathbf{x}(i)$ we can locally approximate F^T to estimate $x(i+T)$ taking into account the k nearest neighbors of $\mathbf{x}(i)$, $\{\mathbf{x}(i(1)), \dots, \mathbf{x}(i(k))\}$. Note that for each target point $\mathbf{x}(i)$ and time step T a different model is computed. In our work, we use three different local approximations of F^T .

a) Local weighted averaging

This is a geometrical nonparametric method implementing the idea that spatially close points have close T-step ahead mappings. So, we take the weighted average of the T-step ahead mappings of the k neighbors. The weighting is with

respect to the distance of each neighbor point from the target point $\mathbf{x}(i)$. Actually, through an iterative process, we find the estimated $\mathbf{x}(i+T)$ to have distance from the mappings $\{\mathbf{x}(i(1)+T), \dots, \mathbf{x}(i(k)+T)\}$ relative to the distance of $\mathbf{x}(i)$ from the k neighbors (Abarbanel et al., 1993; Sugihara and May, 1990).

b) Local Linear Map with Ordinary Least Squares

The local approximation of F^T may be done with a linear map, i.e. $\hat{\mathbf{x}}(i+T) = \mathbf{a}_0 + \mathbf{a}^T \mathbf{x}(i)$. Assuming that this model is good enough for the neighborhood of $\mathbf{x}(i)$, i.e. the above equation yields also for the mapping of the k neighbors, where $k > m$, we can solve a system of k equations with $m+1$ unknown variables, the $m+1$ parameters $\{\mathbf{a}_0, \mathbf{a}\}$ using the ordinary least squares (OLS). The derived parameter values are then used to find the mapping $\hat{\mathbf{x}}(i+T)$. (Farmer and Sidorowich, 1987; Casdagli et al., 1992).

c) Local Linear Map with Regularization of Ordinary Least Squares

The system of equations described above in (b) can be solved differently by introducing certain regularizations on the OLS solution, e.g. requiring reduction of the dimensionality of the parameter space. In this way, more robust solutions can be obtained, especially for large embedding dimension m and for noisy data (Kugiumtzis et al., 1998). Here, we use a simple regularization of OLS using Principal Component Regression (PCR). Using PCR, the dimension reduction is done by considering only the first q of the m principal components, and we denote the method with PCR(q).

2.3 Dynamics and mutual information

Chaotic or stochastic dynamical systems can be described by using the concept of information. For this scope we suppose that the random behavior of the system is a realization of Shannon's concept of an ergodic information source (Shaw, 1981, 1984; Abarbanel et al., 1993). If S is some property of the dynamical system and $\{s_i, i = 1, 2, \dots\}$ possible values of S then the average amount of information gained from a measurement that specifies S is given by the entropy $H(S)$

$$H(S) = \sum_i P(s_i) \log P(s_i) \quad (8)$$

where $P(s_i)$ is the probability that S equals to s_i and it is estimated by $\frac{n(s_i)}{n_T}$, with $n(s_i)$ the number of times that the value s_i is observed and n_T the total number of measurements. The same concept can be used to identify how much information we obtain about a measurement of an observable S from measurement of another observable Q . This concept is the base of the definition of mutual information. For time series, we consider a general coupled system (S, Q) with $Q = \{x(i)\}$ and $S = \{x(i+\tau)\}$, where $x(i), x(i+\tau)$ correspond to the scalar samples from a dynamical system at discrete times t_i and $t_{i+\tau}$. The amount by which a measurement of Q reduces the uncertainty of S (average mutual information) is given by the relation

$$I_{SQ} = H(S) - H(S/Q) = H(S) + H(Q) - H(Q, S) \quad (9)$$

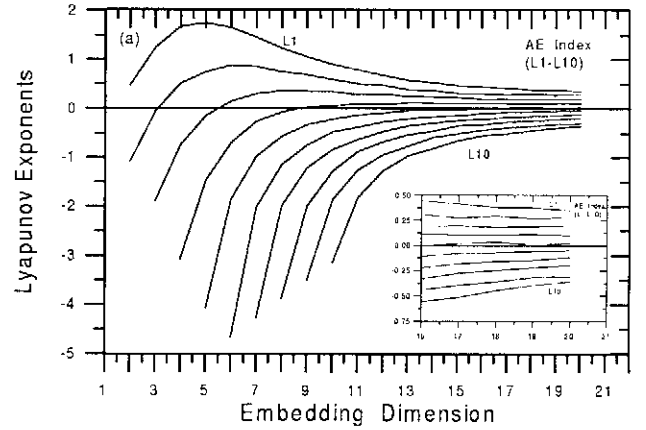


Fig. 1. (a) The spectrum of the first ten Lyapunov exponents estimated for the AE index as a function of the embedding dimension m .

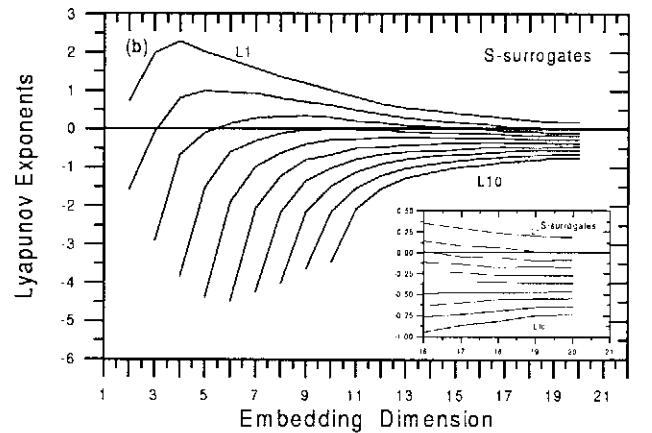
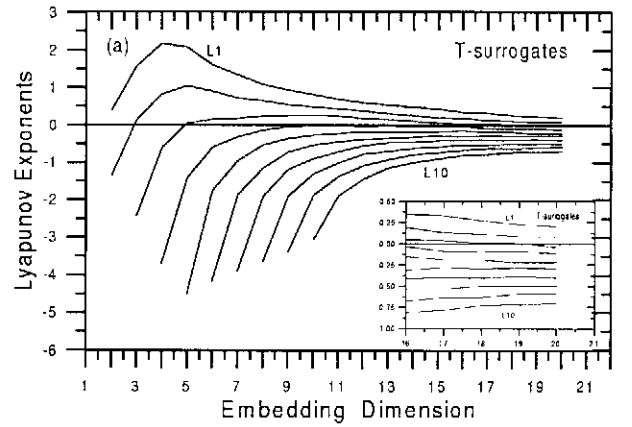


Fig. 2. (a) The spectrum of the first ten Lyapunov exponents for one T-surrogate signal as a function of the embedding dimension m . (b) The same with (a) but for one S-surrogate signal.

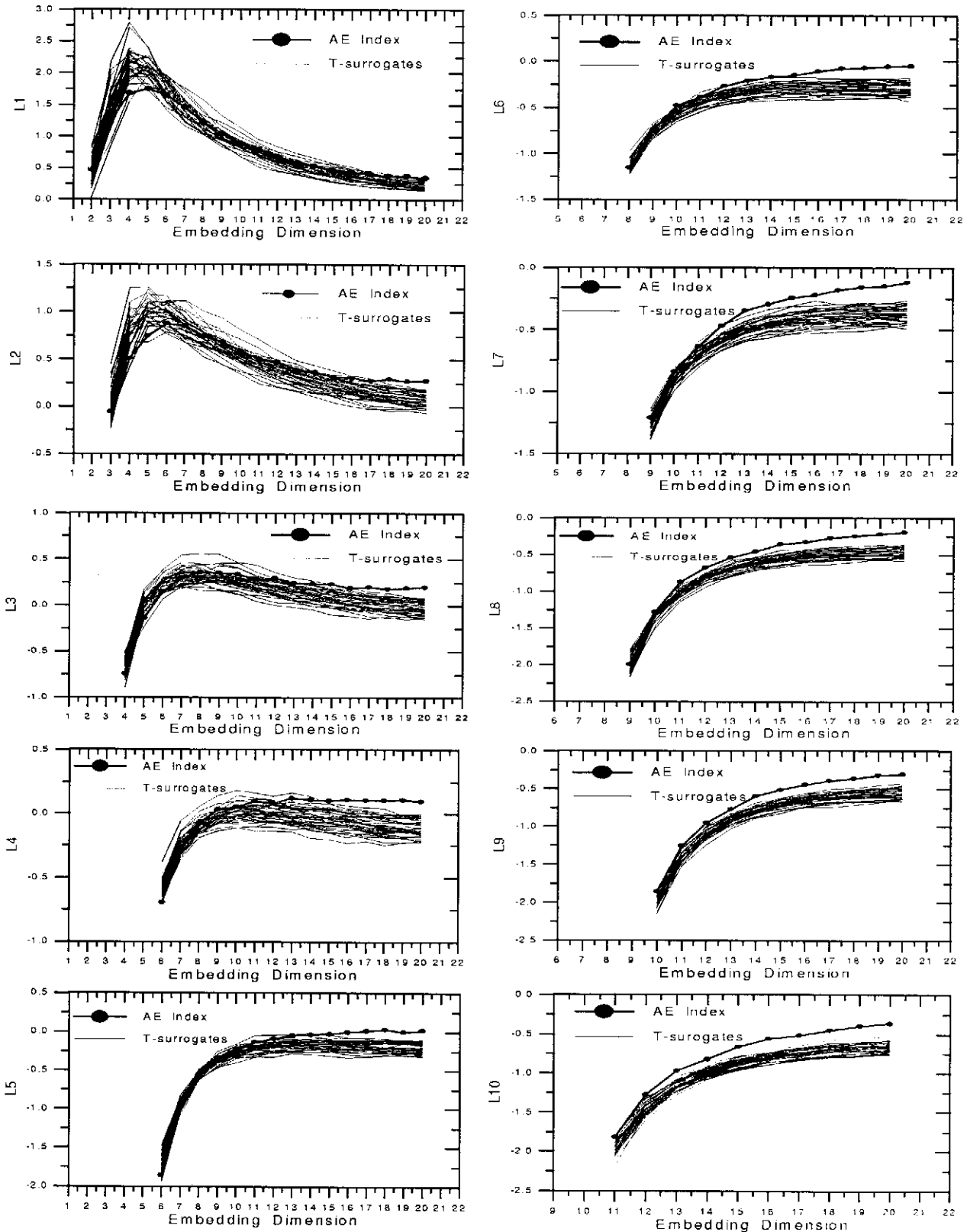


Fig. 3. (a) This figure includes the L_1 - L_{10} Lyapunov exponents for the entire group of T-surrogate data. The corresponding exponents of the AE index are included, too.

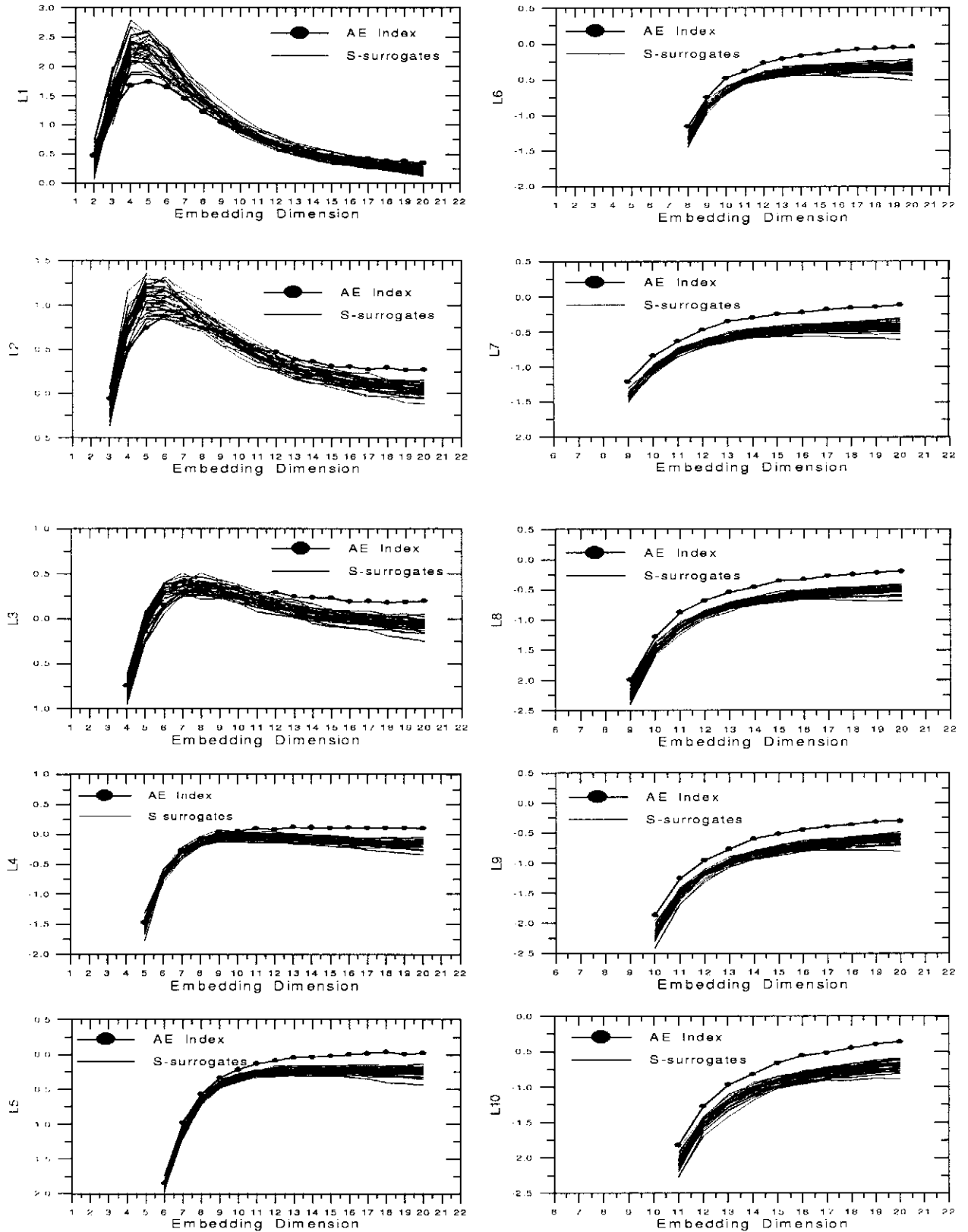


Fig. 4. The same with Fig. 3 but for the S-surrogate data.

and applied to time series leads to

$$\begin{aligned}
 I(\tau) = & - \sum_{x(i)} P(x(i)) \log_2 P(x(i)) \\
 & - \sum_{x(i-\tau)} P(x(i-\tau)) \log_2 P(x(i-\tau)) \\
 & - \sum_{x(i)} \sum_{x(i-\tau)} (P(x(i), x(i-\tau)) \\
 & \times \log_2 P(x(i), x(i-\tau))) \quad (10)
 \end{aligned}$$

The mutual information between the two samples $\{x(i)\}, \{x(i+\tau)\}$ takes values in the range $(0, I_{max})$, where $I_{max} = I(0)$ is equal to the information entropy $H(x)$. If the samples $\{Q \equiv x(i)\}$ and $\{S \equiv x(i+\tau)\}$ are statistically independent then the mutual information will vanish for this τ . That is no knowledge can be gained for the second sample by knowing the first. On the other hand, if the first sample uniquely determines the second sample then $I(\tau) = I_{max}$, which is most likely to be true when $\tau = 0$.

In this work, we follow Fraser and Swinney (1986) in order to estimate the mutual information (according to Eq. (10)) of an experimental time series, which is used as discriminating statistic parameter between the surrogate data and the original time series.

3 Data analysis and results

The AE index describes the Auroral-zone magnetic activity which is related with the global magnetospheric dynamics through a complex system of currents. The magnetospheric dynamics during substorms is manifested as strong variability of the magnetospheric and ionospheric electric currents especially the auroral electrojets. (McPherron, 1995). Disturbances in the Earth's magnetic field produced by currents in the magnetosphere and ionosphere are commonly described by a number of magnetic activity indices, which are derived from certain physical parameters connected to the dominant phenomena causing the disturbance. The indices AU, AL, and AE give a measure of the strength of the auroral electrojets and are defined with the use of traces of the horizontal component (H) of the geomagnetic field measured by a world-wide chain of auroral-zone magnetic observatories (Davis and Sugiura, 1966). AU is the maximum positive disturbance (upper envelope) recorded by any station in the chain. AL is the minimum disturbance defined by the lower envelope of the traces of the chain. AE is defined by the separation of the envelopes ($AE = AU - AL$) in order to obtain a better measure of the strength of the auroral electrojets. The sampling rate of the original signal was one minute while the time series used in this paper contains $N_T = 32768$ data points that are the eight minute averages of the entire time series, rounded to the nearest power of two. That is the original time series contains $N \cong 250.000$ data points. This time series has much longer length than the time series used in our previous work (Pavlos et al., 1992b, 1994) as well as in the work of other scientists.

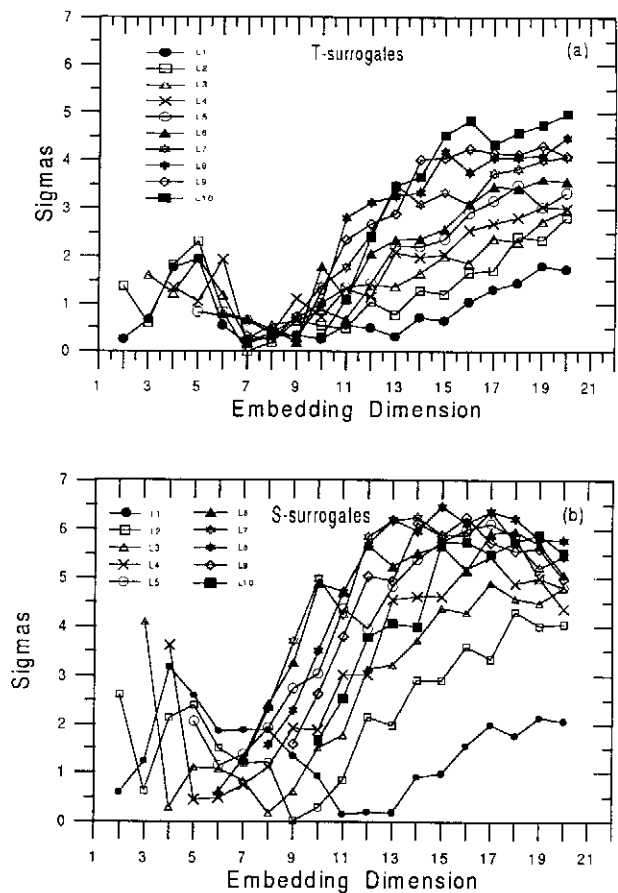


Fig. 5. (a) The significance of the discriminating statistics of the Lyapunov exponents as a function of the embedding dimension m corresponding to the T-surrogate data. (b) The same with (a) for the S-surrogate data.

In the following we present the results about the dynamical characteristics of the AE index time series and the corresponding discriminating statistics for its surrogate data.

3.1 Spectrum of Lyapunov exponent

The spectrum of Lyapunov exponents was estimated with the algorithm presented in Sect. 2.1. Figure 1 shows the first ten Lyapunov exponents (L-exponents) estimated for the AE index time series for different embedding dimensions m . The L-exponents saturate as m increases as shown at the enlargement in Fig. 1. The first four exponents ($L_1 - L_4$) take positive final values, L_5 is close to zero, and the remaining ones take negative values. For a purely deterministic system the existence of positive L-exponents implies chaotic dynamics, but for a signal contaminated by noise it is possible some L-exponents can be positive due to the stochastic perturbation. It is known that stochastic data give often positive L-exponents without the underlying dynamics necessarily being chaotic (Osborne et al., 1986; Provenzale et al., 1991; Argyris et al., 1998a).

When the embedding dimension is larger than the degrees of freedom of the underlying system spurious exponents oc-

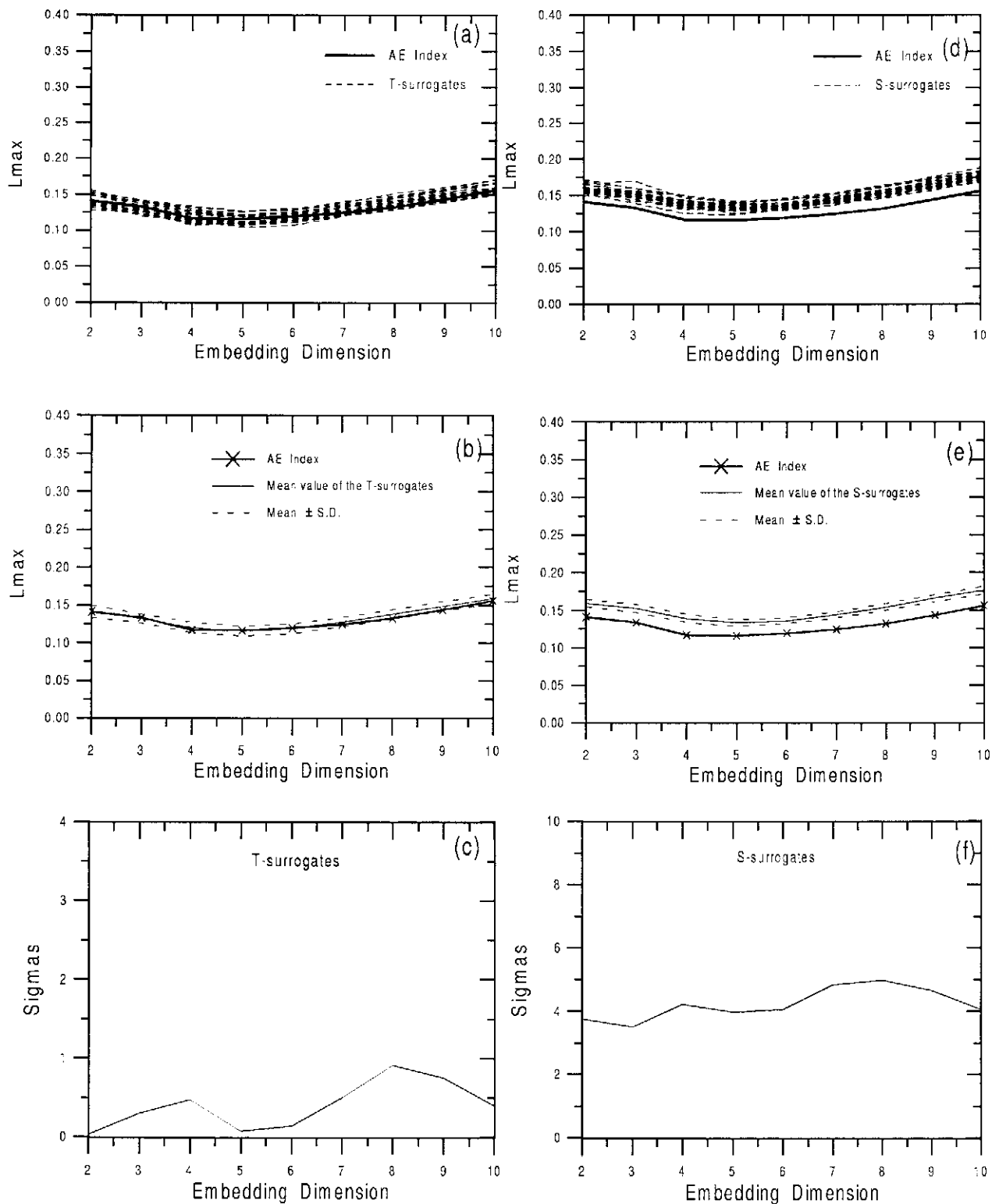


Fig. 6. (a) The largest Lyapunov exponent (L_{max}) estimated for the T-surrogate data and the AE index as a function of the embedding dimension m . (b) The L_{max} for the AE index, the mean value and S.D. of L_{max} for the T-surrogate data shown in (a). (c) The significance of the L_{max} discriminating statistic as a function of m . (d-f) The same with (a-c) but for the S-surrogate data.

cur as an artifact of the embedding, but the existence of more than one positive L-exponents for the AE index time series, constitutes significant evidence that at least one of them could correspond to the underlying deterministic dynamics. In order to verify the validity of this statement we estimate the Lyapunov spectrum also for the surrogate data according to the null hypothesis that the AE time series belongs to a family of linear stochastic signals transformed by a nonlinear static distortion. As in Part I (Pavlos et al., 1999a) in the following we make use of two kinds of surrogate data, the T-surrogate as presented in (Theiler et al., 1992a) and the S-surrogate, as presented in (Schreiber and Schmitz, 1996) which mimic the AE index time series in relation to the amplitude distribution and the autocorrelation function. Figures 2a-b show the spectrum of L-exponents for two "nonlinear" T and S-surrogate data. The number of positive L-exponents is clearly lower than those of the original AE index time series as we have 2 positive L-exponents in the case of T and S-surrogate data. In order to obtain more convincing results we created a rich statistic of both T and S surrogate signals including 40 surrogate data in each case as shown in Figs. 3 and 4, respectively. In both cases of surrogate data each L-exponent of the AE index time series obtains larger values than those of the surrogate data when m is large except for L_1 , which is marginally larger than the corresponding exponent for the surrogates. The significance of the discriminating statistics of L-exponents is presented in Figs. 5a-b. It is obvious that for large m the significance of the statistics becomes higher than two sigmas for all the exponents except the first (L_1). For L_1 the significance is marginally lower than 2 sigmas for T-surrogate and marginally greater than 2 sigmas for S-surrogate. In general, the significance of the statistics for the S-surrogate data for all L-exponents are sensibly higher than for the T-surrogate data.

The largest Lyapunov exponent L_{max} has been estimated independently according to the Eq. (6). The results of this estimation for the AE index and its surrogate data are shown in Fig. 6. For L_{max} the discrimination between the original time series and its T-surrogate data is impossible, as the significance of the statistics remains lower than 2 sigmas for m in the range 2-10 (see Figs. 6a-c). On the other hand, for the S-surrogate data the discrimination is possible as the significance of the statistic remains higher than two sigmas, fluctuating at the range of 3-5 sigmas (see Figs. 6d-f). The above results for the L-exponents spectrum as a discriminating statistics clearly permit the rejection of the null hypothesis with confidence greater than 95%.

3.2 Modeling and prediction

In the following we present the results of the hypothesis test using the prediction and modeling methods described in Sect. 2.2. In particular, we use three local linear prediction models as well as global linear and nonlinear polynomial fitting. The performance of the models on linear stochastic signals depends solely upon the autocorrelation function of the signals. Figure 7 shows the autocorrelation coefficient of the

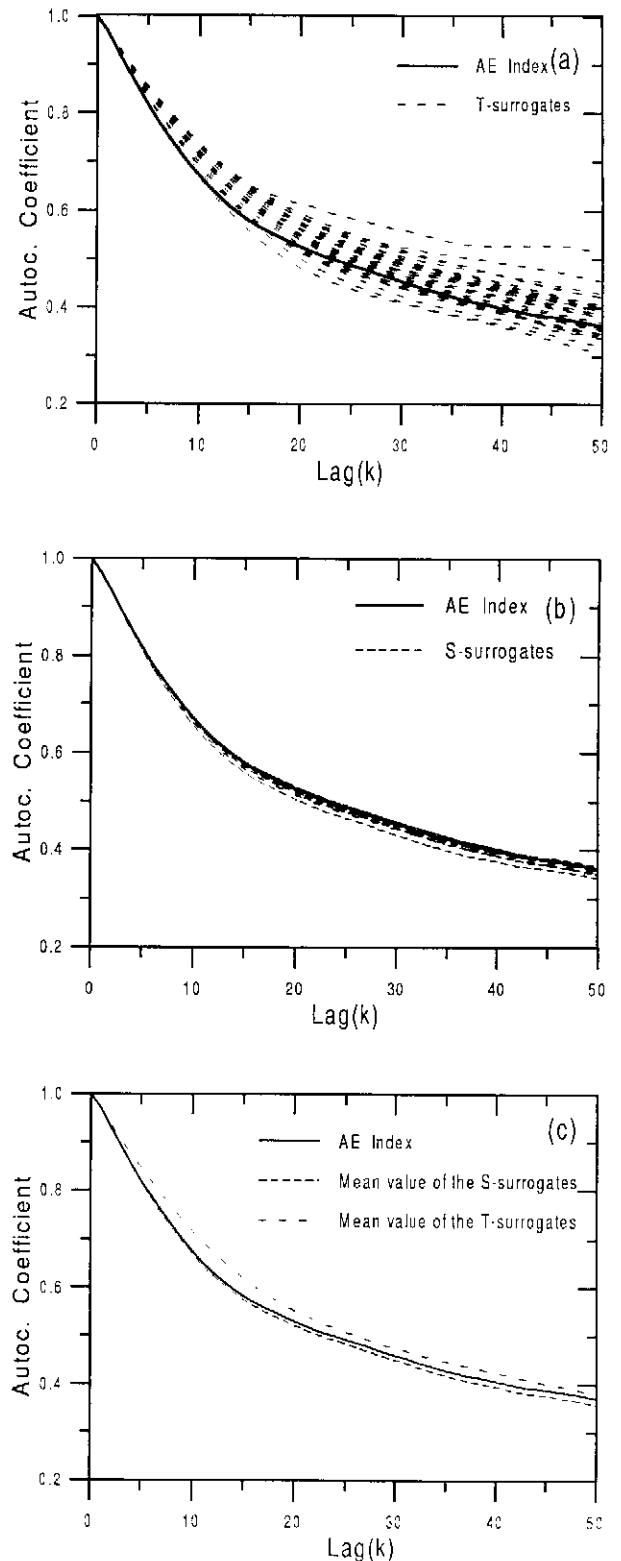


Fig. 7. (a) The autocorrelation function estimated for the AE index and for a group of 40 T-surrogate data. (b) The same with (a) but for a group of 40 S-surrogate data. (c) The autocorrelation function of the AE index and the mean value of the autocorrelation functions of the surrogates shown in (a) and (b) of this figure.

AE index time series and its surrogates, estimated for the first 50 lags. The autocorrelations for the T-surrogates and the S-surrogates are shown in Fig. 7a and in Fig. 7b, respectively. Figure 7c reveals the difference between the autocorrelation of the AE index and the mean values of the autocorrelations of the surrogates. In this figure it is apparent that the autocorrelations of the S-surrogates mimic the AE index autocorrelation much better than the T-surrogates. However, a weak deviation of the S-surrogate autocorrelations from the AE index autocorrelation is also observed, especially for lags larger than 10 time units. It is obvious that statistically the autocorrelation values for T-surrogates are larger than the AE index autocorrelation values. Moreover, the observed deviation of the autocorrelation mean value of the S-surrogates from the corresponding mean values of the AE index is much smaller and of opposite sign than that for T-surrogates. These discrepancies in autocorrelation turn out to have major impact on the results we present below.

3.2.1 Non parametric local linear prediction

Figure 8 displays the results of the prediction with local weighted averaging on the AE index and its surrogate data, as presented in Sect. 2.2.2. For the estimation of the prediction we used for the embedding space $m = 7$ and delay time $\tau = 1$, $k = m + 1$ neighbors, as training set the first 24000 values and as test set the rest 8000 values of the time series. The correlation coefficient (CC) for $T = 1 - 20$ step ahead predictions for the AE index and its 40 T-surrogates are shown in Fig. 8a. Figure 8b shows the mean value and standard deviation of CC for the T-surrogates together with the CC for the AE index. The significance of the above statistics is shown in Fig. 8c. The small values of the significance (0.0 – 0.75) shows that there is no significant discrimination between the original time series and its surrogates. Figures 8d-f are similar to Figs. 8a-c corresponding to the S-surrogates. In these figures we observe the same result as that obtained for the T-surrogates.

The above results reveal that it is not possible to reject the null hypothesis by using this nonparametric linear prediction scheme. We suspect that the predictability of AE and its surrogates is strictly determined by the autocorrelation function, in such a way that coincidence of the autocorrelations leads to the same predictability. While the above results suggest that it is not possible to discriminate between the AE index and its surrogates but they do not also prove also the linearity of the AE index. While strongly nonlinear and noise-free signals are successfully discriminated from the surrogates (as the predictability is less dependent upon the autocorrelation), for nonlinear signals with weak nonlinearity or strong noisy component this may not be possible.

3.2.2 Parametric local linear prediction

In this case we have followed two methods of local linear prediction (LLP). That is we estimate the local linear maps using ordinary least square fitting (OLS) and the regulariza-

tion of OLS with principal components regression (PCR), as presented in Sect. 2.2.2. Figure 9 presents the results of LLP with OLS fitting for (T) and (S) surrogate data and Fig. 10 does the same for LLP with PCR regularization. For the estimations we used embedding dimension $m = 10$, delay time $\tau = 1$, $k = 60$ neighbors, and for regularization parameter $q = 3$. For the T-surrogates, the statistics tend to be significant for small T ($T \leq 4$) (see Fig. 9c and Fig. 10c), especially in the first case of LLP with OLS. This result is apparently caused by the deficiency of T-surrogates to mimic faithfully the autocorrelation of the AE index. This is supported by the small significance of the same statistics estimated for the S-surrogate data (in the range 0-1 sigma as shown in Fig. 9f and Fig. 10f). The above result for the S-surrogate data was somehow expected as the autocorrelations of the S-surrogates mimic the autocorrelation of AE index more faithfully than the T-surrogates. Therefore, we conclude that in both cases of parametric local linear prediction it is also impossible to discriminate the original time series from its surrogate data. We note also that the dependence of the local parametric prediction models on the autocorrelation seems to be larger than for the local nonparametric models.

3.2.3 Global linear and nonlinear polynomial fitting

The modeling with global polynomials gave good discrimination between the original and surrogate data, especially when we defined the discrimination statistic to be the change of the modeling error as we go from linear to non linear polynomial terms. Here, we use the NRMSE to quantify the modeling error and we consider 5 steps ahead mappings from all the polynomials of the Volterra Wiener series, as presented in Sect. 2.2.1.

In Fig. 11a the NRMSE for 40 T-surrogate data and the AE index is shown as a function of the polynomial terms of the Volterra Wiener series, using $m = 10$ and $q = 2$ (see Eq. 7). The first 11 polynomial terms are linear (the first term is the constant) and the rest are nonlinear interactions of the 10 delays. Figure 11b shows the mean value of NRMSE and its standard deviation for the T-surrogates together with NRMSE of the AE index. Obviously, NRMSE for the AE index is statistically larger than for the T-surrogates. This is observed even for maps with only linear terms, for which the coincidence of the errors is expected because the predictability is determined entirely by the autocorrelation of the signal. The observed discrepancy in NRMSE is due to the difference between the autocorrelations of the T-surrogates and the AE index according to Fig. 7a and Fig. 7c. For linear signals, the autocorrelation determines the predictability in such a way that signals with larger autocorrelation values reveal larger predictability and smaller prediction error. Since the above result is also observed also for the nonlinear polynomial terms, the supposed nonlinearity of the AE index is either weak or covered by a strong noise component. However, the existence of noticeable nonlinearity for the AE index is proved by the abrupt reduction of the AE index error as we pass from the linear to the nonlinear fitting, as shown

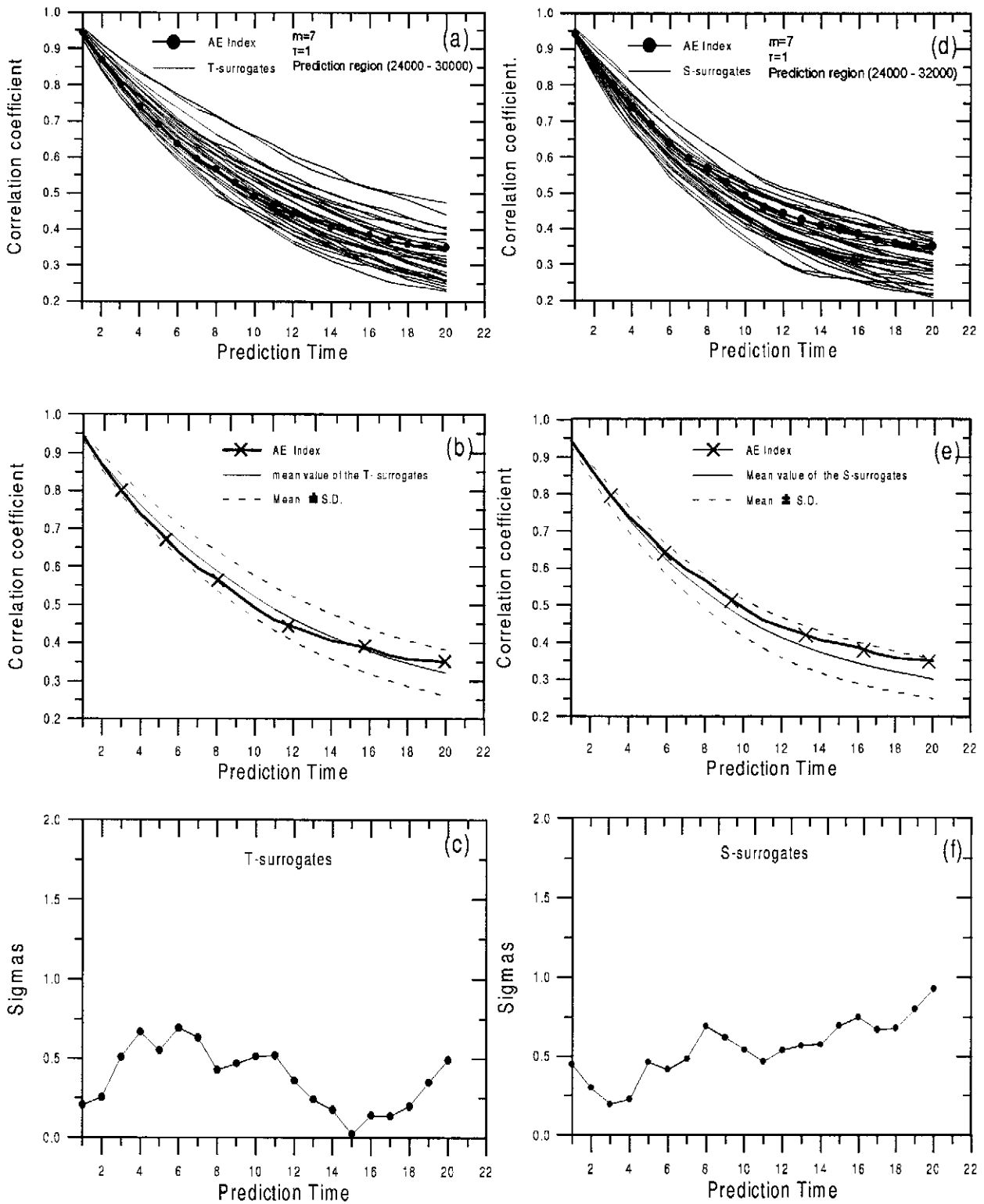


Fig. 8. (a) Correlation coefficient between predicted and real values for the T-surrogate and the AE index estimated using the local weighted averaging. (b) The mean value and S.D. of the correlation coefficients for the T-surrogate data shown in (a) together with the correlation coefficient for the AE index. (c) Significance of the discriminating statistics shown in (a). (d-f) The same with (a-b) but for the S-surrogate data.

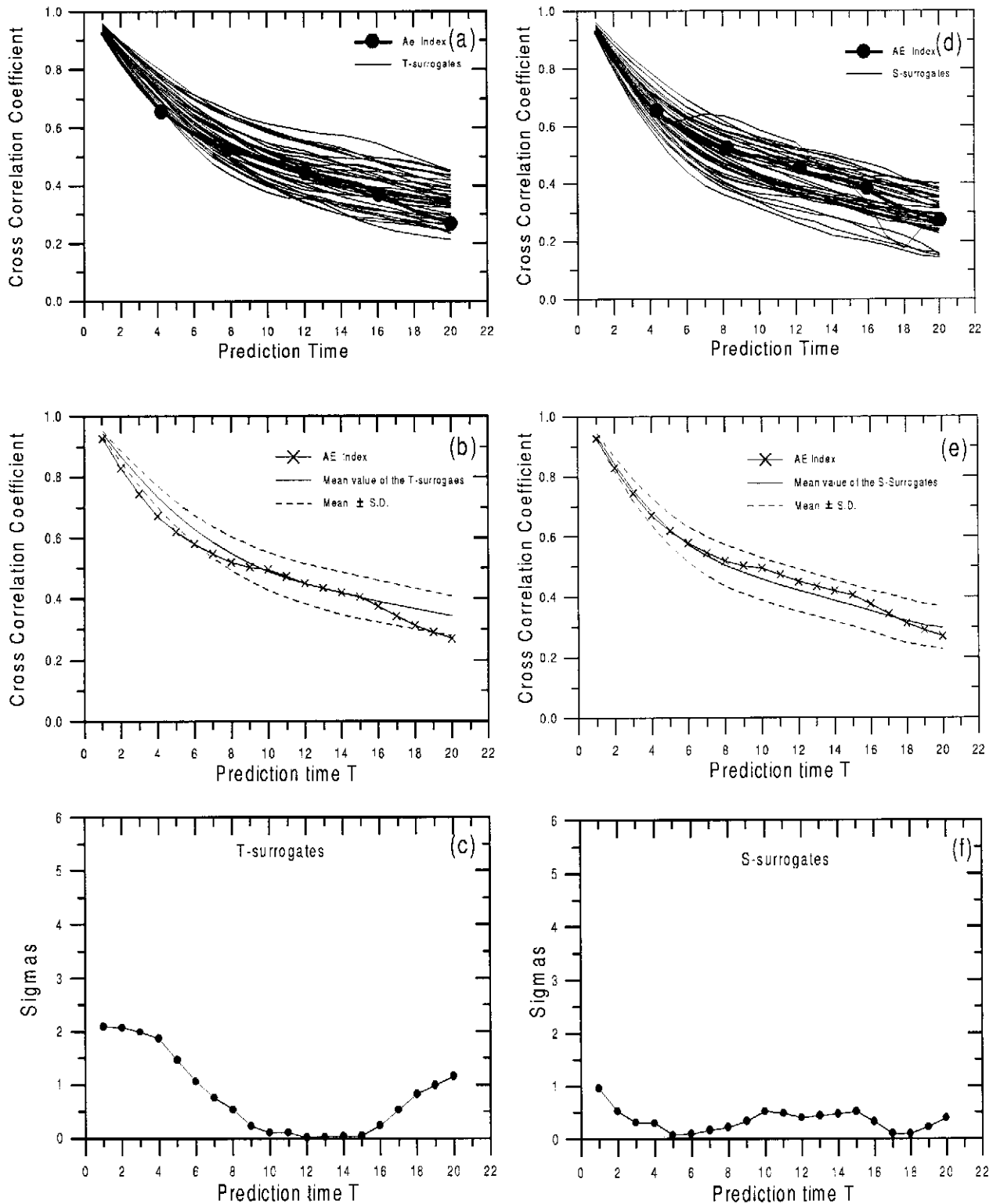


Fig. 9. The same with Fig. 8 but for parametric local linear prediction (LLP) with ordinary least squares (OLS).

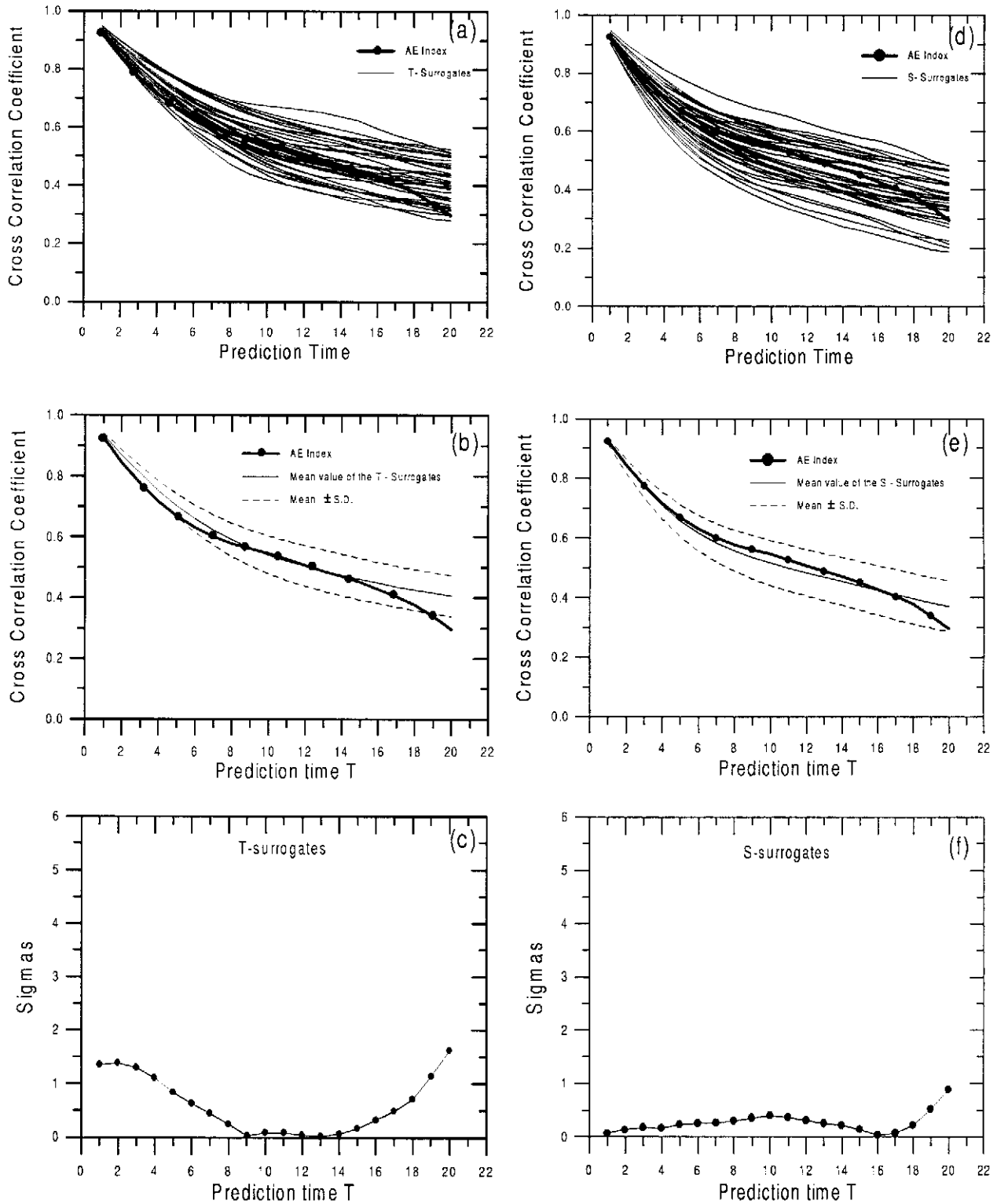


Fig. 10. The same with Fig. 8 but for parametric LLP using the regularization technique of principal components regression (PCR).

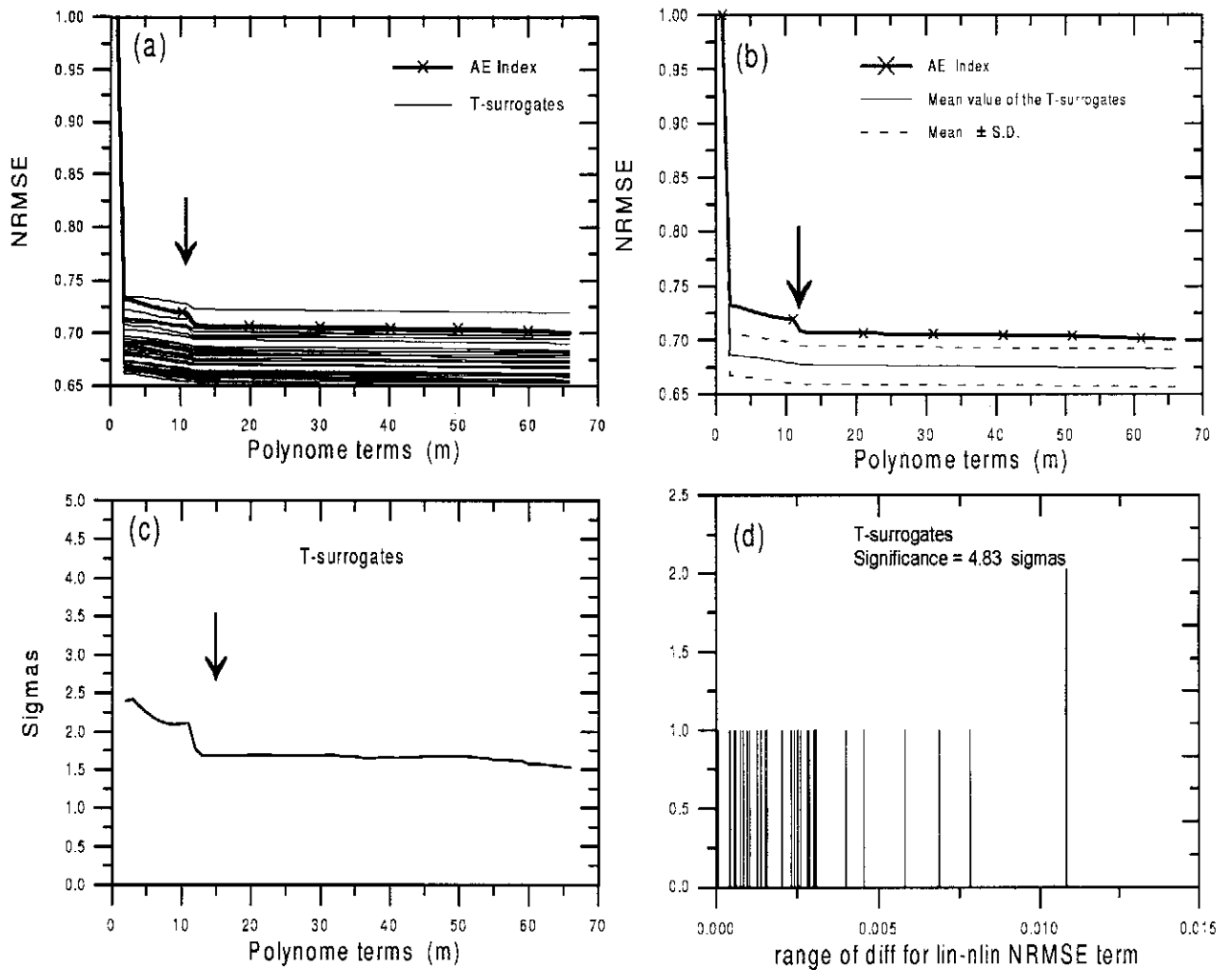


Fig. 11. (a) Normal root mean squares error (NRMSE) estimated by using polynomial fitting for the AE index time series and T-surrogate data signals as a function of the polynomial terms. The first ten terms are linear and the next terms are non linear. (b) The same with (a) for the AE index and the mean value and S.D. of NRMSE corresponding to the statistics shown in (a) of this figure. (c) The significance of the NRMSE statistic as a function of the polynomial terms. (d) The discriminating statistic of the error reduction at the first nonlinear term (12th term) for the AE index (tall line) and the T-surrogate data (short lines). The error reduction is indicated by the vertical vector in pictures (a, b, c).

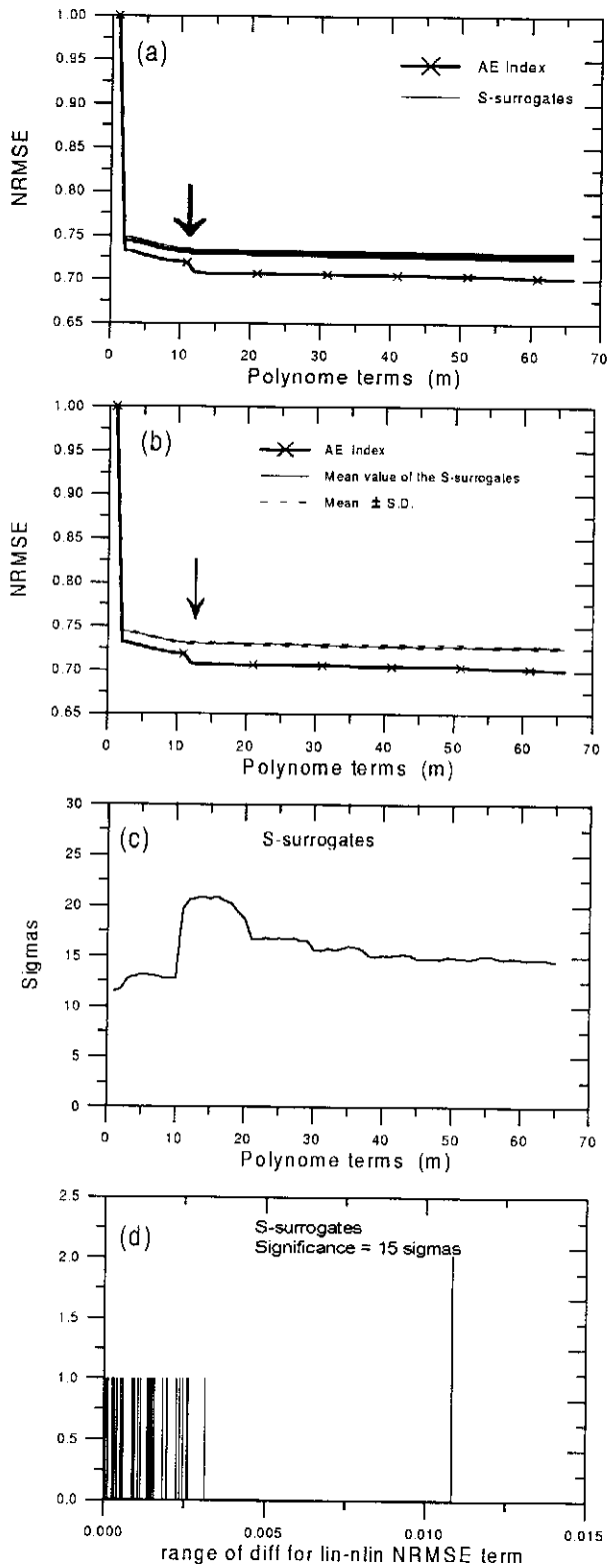


Fig. 12. The same with Fig. 11 but for the S-surrogate data.

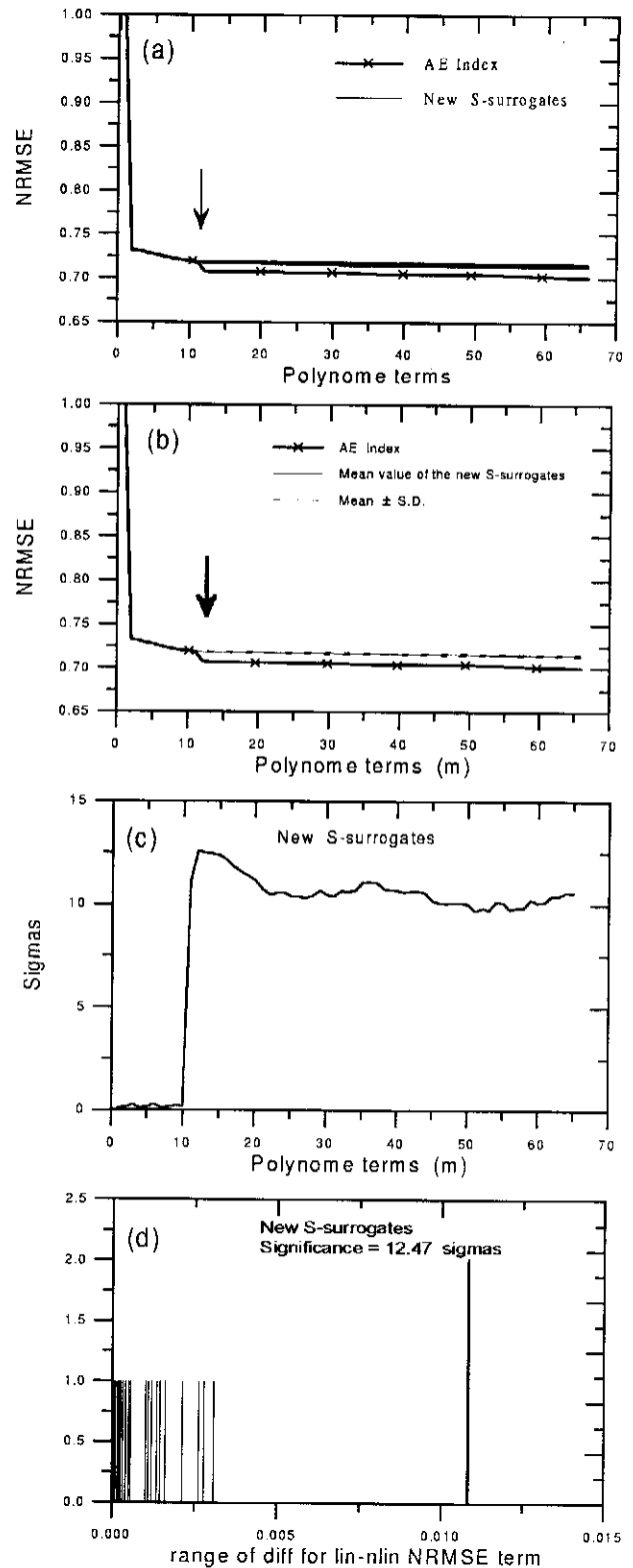


Fig. 13. The same with Fig. 11 but for the new S-surrogate data (see text).

in Figs. 11a-b by the difference of NRMSE from 11 to 12 terms. This feature is almost absent for the T-surrogates.

Figure 11c shows the significance of NRMSE statistic for the linear and nonlinear terms of the polynomial fitting. For linear terms the significance of the statistic reveals values larger than 2 sigmas, while for nonlinear terms the significance varies at smaller values in the range 1.5 – 2.0 sigmas. The large values of the significance at the linear region is an artifact caused by the difference between the autocorrelations of the surrogates and the AE index. To the contrary, the abrupt decay of the NRMSE by introducing the nonlinear terms in the polynomial fitting leads to a reliable discrimination between the AE index and its T-surrogates, giving significance at about 5 sigmas, and constitutes strong evidence for the nonlinearity of the AE index time series (see Fig. 11d).

In the case of S-surrogate data the discrimination power of the global polynomial fitting is more intensive. Figure 12 is similar to Fig. 11 and corresponds to S-surrogate data. The NRMSE takes larger values for the S-surrogates than for the AE index, both for linear and non-linear fitting. This is again due to the difference of the autocorrelations, i.e. for the S-surrogates the autocorrelations are slightly smaller than for the AE index (Fig. 7c). The significance of the NRMSE statistic, shown in Fig. 12c, is ~ 12 sigmas for the linear terms and increases to ~ 20 sigmas when the first nonlinear term is entered, and remains at large values for the next nonlinear terms. The abrupt increase of the significance of the statistics at the first nonlinear term and its large values for all the nonlinear terms strongly supports the non-linearity of the AE index, permitting the rejection of the null hypothesis. This conclusion is supported also by the error reduction adding the first nonlinear term estimated for the AE index and its surrogates. This discriminating statistic, shown in Fig. 12d, gives significance ~ 15 sigmas while for the T-surrogates it was found ~ 5 sigmas.

Now, we show that the discrepancy in NRMSE for the linear terms is solely due to discrepancy in autocorrelation. To achieve an exact matching in autocorrelation we let the algorithm of Schreiber and Schmitz converge completely, i.e. until the reordered stochastic signal does not change for the consequent iterations (in the cost of large computation time). The new results are shown in Fig. 13. The deviation in NRMSE for the linear terms has been now removed and the significance of the NRMSE statistic for the linear terms has fallen to zero. On the other hand, the significance rises to over 10 sigmas as the first nonlinear term is introduced and stays at the 10 sigmas level for all nonlinear terms. The significance of the NRMSE after adding the first nonlinear term has been estimated to ~ 13 sigmas (see also Fig. 13d).

The above results about the polynomial fitting especially for the S-surrogates strongly reject the null hypothesis and support faithfully the nonlinearity of the AE index time series, with confidence $> 95\%$.

3.3 Mutual Information

Mutual information for the AE index and its surrogate data has been estimated implementing algorithmically the definition (10) in Sect. 2.3. Figure 14a shows the mutual information estimated for the AE index and its T-surrogates as a function of the lag time τ . Figure 14b shows the mean value and the standard deviation of the statistics together with the mutual information of the AE index. The mutual information for the AE index is slightly larger than that for the T-surrogates. This difference is significant enough for the discrimination between the AE index and its surrogate data (Fig. 14c). Especially for smaller τ , e.g. the first 20 lags, the significance obtains values in the range of $\sim 2 - 12$ sigmas. For the larger lags the significance fluctuates in the region $\sim 0 - 4$ sigmas. The above results permit us to reject the null hypothesis and support the nonlinearity of the AE index. Actually, the difference in mutual information is larger if we take into account that T-surrogates have larger linear correlations than the AE index (see also Fig. 7a and Fig. 7c).

Figures 14d-f are similar to Figs. 14a-c and correspond to the S-surrogate data. Now, the values of mutual information of AE index are clearly larger than the corresponding values of the S-surrogates (see Figs. 14d-e). The significance of the statistics for the first 20 lags was estimated to be in the region $\sim 5 - 12$ sigmas and clearly larger than 2 sigmas for higher lags, apart from few distinct lags. Comparing the mutual information of the S and T surrogates (see Fig. 14b and Fig. 14e) we see that the mutual information for the S-surrogates is smaller in average than for the T-surrogates. This result is expected, because for linear signals the mutual information is analogous to the autocorrelation and the autocorrelation for the S-surrogates is smaller in average than for the T-surrogates (see Fig. 7c). On the other hand, the deviation of the mutual information for the S-surrogates from the original, shown in Fig. 14e, is much larger than the corresponding deviation for the T-surrogates, shown in Fig. 14b. This also suggests the nonlinearity of the AE index. Finally, the above comparison of the AE index and its surrogates using as discriminating statistic the mutual information permits us also to reject the null hypothesis with sufficient confidence, larger than 95%.

4 Summary and discussion

In this second part of our study we have tested the null hypothesis that the dynamical characteristics of the AE index time series are similar with those of linear stochastic signals. We considered stochastic signals that are supposed to mimic the amplitude distribution and the power spectrum (or equivalently the autocorrelation function) of the AE index after a nonlinear static distortion. For this testing we used two different schemes for the generation of surrogate data according to Theiler et al. (1992b,a) (T-surrogates) and Schreiber and Schmitz (1996) (S-surrogates). It turned out that the S-surrogate data can mimic the autocorrelation function of the

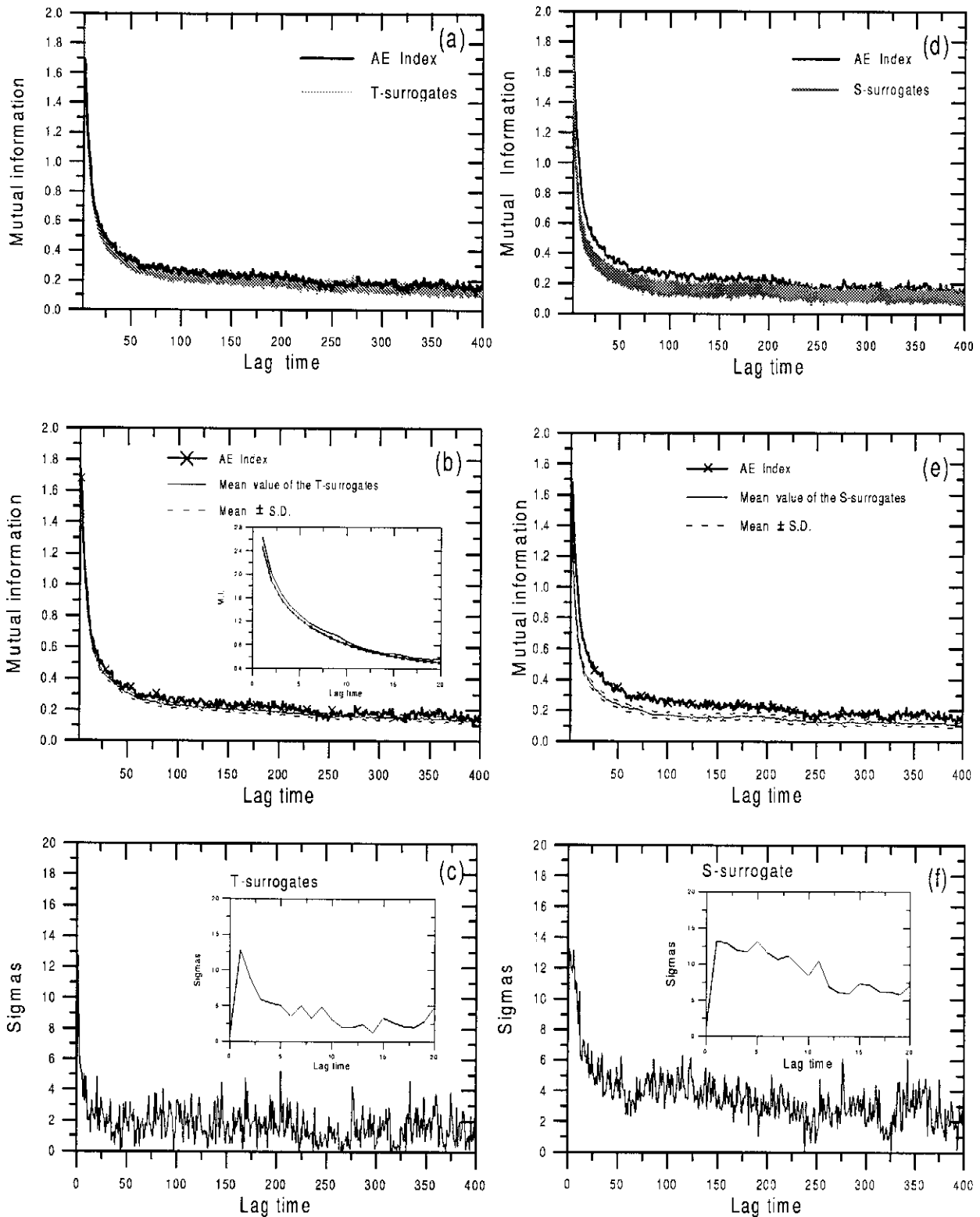


Fig. 14. (a) Mutual information estimated for the AE index and for the T-surrogate data as a function of the lag time. (b) The same with (a) but for the AE index and the mean value and S.D. for the T-surrogate data shown in (a). (c) Significance of the discriminating statistic of mutual information of the T-surrogate data, as a function of lag time. (d-f) The same with (a-c) but for the S-surrogate data.

Table 1. This table summarizes the L-exponents spectrum of the AE index at $m = 20$ (column 2) and the mean values of L-exponents for the surrogate data (columns 3 and 4), as well as the significance of the corresponding discriminating statistics (columns 5 and 6). The last row is for the maximum Lyapunov exponent estimated independently for $m = 10$.

L.E.	AE - index	Spectrum of Lyapunov exponents		"Nonlinear" surrogate data	
		T-surrogate data (mean values)	S-surrogate data (mean values)	T - surrogate data (sigmas)	S-surrogate data (sigmas)
L_1	0.346	0.243	0.240	1.73	2.06
L_2	0.277	0.083	0.035	2.81	4.05
L_3	0.199	-0.014	-0.073	2.97	4.80
L_4	0.093	-0.102	-0.162	2.99	4.37
L_5	0.022	-0.189	-0.250	3.33	4.81
L_6	-0.051	-0.279	-0.339	3.57	5.08
L_7	-0.118	-0.365	-0.426	4.08	5.45
L_8	-0.196	-0.456	-0.516	4.48	5.77
L_9	-0.306	-0.553	-0.608	4.09	4.99
L_{10}	-0.360	-0.652	-0.704	4.98	5.51
L_{max}	0.155	0.160	0.175	0.45	4.00

Table 2. This table includes the significance of the discriminating statistics of polynomial fitting (linear and nonlinear) given by NRMSE for the T-surrogates and for the two groups of S-surrogates. The significance of the error reduction passing from linear to nonlinear terms of the polynomial fitting is also shown.

NRMSE for polynomial fitting	Significance of the statistics		
	T-surrogate data (sigmas)	S-surrogate data (sigmas)	
		Partial convergence	Complete convergence
Linear fitting	2-2.5	11-13	< 1
Nonlinear fitting	~ 1.5	15-21	10-12
Error reduction	5	15	12.47

AE index better than the T- surrogate data. This difference between S and T-surrogate data is manifested in the discriminating statistics we used to test the null hypothesis.

For the Lyapunov spectrum and the polynomial fitting the significance of the statistics is larger for the S-surrogates, but smaller in general for local linear prediction. Therefore, we conclude that the S-surrogate data are more suitable for testing the null hypothesis especially when we let the algorithm which generates them converge completely.

The estimated values of the L-exponents for the AE index and the significance of the corresponding statistics are summarized in Table 1. This table shows that for the AE index there were estimated four positive L-exponents while for the T-surrogate and S-surrogate data only two. The significance of the L-exponent discriminating statistic is systematically larger for the S-surrogates than for the T-surrogates and much larger than 2 sigmas, especially for S-surrogates. These results permit us to reject the null hypothesis using the L-exponents and to suppose that at least one of the four positive L-exponents is not spurious or due to noise in the AE data. If this is correct then the positive L-exponent must be assigned to the deterministic component of the underlying process and, thus, the hypothesis of magnetospheric chaos can be supported from our results on Lyapunov exponents.

We believe that nonlinearity is well documented also by the results from the polynomial fitting, summarized in Table 2. The S-surrogate data generated from the complete convergence of the algorithm give the most proper results for linear fitting (significance down to zero level). Adding non-

linear terms, the difference in NRMSE of the AE index and these S-surrogate data increases abruptly and the significance reads ~ 10 sigmas. These characteristics were found to be absent for T-surrogate data. However, using as discriminating statistic the reduction error after adding the first nonlinear term, high level of discrimination is achieved for all surrogate types. This is due to the improvement of the predictability of the AE index after adding a nonlinear term, even if the decrease of NRMSE is only $\sim 2\%$. Thus, the polynomial fitting is a simple and efficient method for detecting dynamical nonlinearity.

The nonlinearity of the underlying to the AE index determinism was also supported by the estimation of the mutual information, as summarized in Table 3. For surrogate data (of S and T type) the mutual information is determined by the autocorrelation. Comparing the mutual information of the AE data and its surrogates we conclude that for the AE index the mutual information does not depend upon the autocorrelation, which gives again evidence for nonlinearity. Indeed, the significance for the mutual information was found to be much larger than 2 sigmas, especially for the S-surrogates and for small lags (see Table 3).

For signals with weak nonlinearity or with a strong component of noise the nonlinear local prediction is inefficient to discriminate the original signal from its surrogates. This is concluded after applying local prediction methods to the AE index. The negative results on the significance of this discriminating statistic, summarized in Table 4, are in contrast with the previous results of this study which have shown

Table 3. This table shows the significance of the discriminating statistic of the mutual information for different lags and for T and S surrogate data.

Mutual Information for different lag time	Significance of the statistics	
	T-surrogate data (sigmas)	S-surrogate data (sigmas)
1-5 lags	2-12	12-13
5-20 lags	2-5	5-12
20-400 lags	0-4	2-6

Table 4. This table shows the significance of the statistic of the correlation coefficient for the predicted and real values estimated by different types of local models.

Nonlinear local prediction (Correlation coefficient)	Significant of the statistics	
	T-surrogate (sigmas)	S-surrogate (sigmas)
Local Weighted Averaging	0.0-0.7	0.2-1.0
LLP with OLS	0.0-2.0	0.0-1.0
LLP with PCR	0.0-1.7	0.0-1.0

strong confidence (over 95%) for rejecting the null hypothesis. This indicates either the existence of weak nonlinearity of the AE index or the existence of a strong component of noise which can cover partially or globally the nonlinearity in the case of local prediction.

Finally, we believe that the results in Part I (Pavlos et al., 1999a) as well as those in this part constitute significant evidence for low dimensionality, nonlinearity and chaoticity of the underlying physical process to the AE index time series. However, it is known that the magnetospheric system, the dynamics of which is measured through the AE index, is continuously coupled with the external dynamics of the solar wind system. For this reason it remains an open problem the relation of the low dimensional, nonlinear and probably chaotic character of the AE index, as indicated in this study, with the magnetospheric dynamics and its external coupling. In another study (Pavlos et al., 1999b) we encounter this persistent problem about the magnetospheric dynamics and nonlinear analysis of the magnetospheric data.

Acknowledgements. We thank Prof. A. G. Rigas for having kindly read our manuscript and for making constructive comments.

References

- Abarbanel, H. D., Brown, R., Sidorowich, J. J., and Tsimring, L. S., The analysis of observed chaotic data in physical systems, *Rev. Mod. Phys.*, **65**, 1331-1392, 1993.
- Argyris, J., Andreadis, I., Pavlos, G., and Athanasiou, M., The influence of noise on the correlation dimension of chaotic attractors, *Chaos, Solitons, Fractals*, **9**, 343-361, 1998a.
- Argyris, J., Andreadis, I., Pavlos, G., and Athanasiou, M., On the influence of noise on the largest lyapunov exponent and on the geometric structure of attractors, *Chaos, Solitons, Fractals*, **9**, 947-958, 1998b.
- Baker, D. N., Klimas, A. J., McPherron, R. L., and Bucher, J., The evolution from weak to strong geomagnetic activity: an interpretation in terms of deterministic chaos, *Geophys. Res. Lett.*, **17**, 41-44, 1990.
- Bargatze, L. F., Baker, D. N., McPherron, R. L., and Hones, E. W., Magnetospheric impulse response for many levels of geomagnetic activity, *J. Geophys. Res.*, **90**, 6387-6394, 1985.
- Casdagli, M., Jardin, D. D., Eubank, S., Farmer, J. D., Gibson, J., Hunter, N., and Theiler, J., Non linear modeling of chaotic time series: Theory

- and applications, in *Applied Chaos*, edited by H. Kim and J. Stringer, chap. 15, pp. 335-380, John Wiley and Sons, 1992.
- Davis, T. N. and Sugiura, M., Auroral electrojet activity index ae and its universal time variation, *J. Geophys. Res.*, **71**(3), 785-801, 1966.
- Eckman, J. P., Kamphorst, S. O., Ruelle, D., and Ciliberto, S., Liapunov exponent from time series, *Phys. Rev. A*, **34**, 4971-4980, 1986.
- Eckmann, J. P. and Ruelle, D., Ergodic theory of chaos and strange attractors, *Rev. Mod. Phys.*, **57**, 617-628, 1985.
- Farmer, D. J. and Sidorowich, J. J., Predicting chaotic time series, *Phys. Rev. Lett.*, **59**, 845-848, 1987.
- Fraser, A. M. and Swinney, H., Independent coordinates for strange attractors from mutual information, *Phys. Rev. A*, **33**, 1134-1140, 1986.
- Holzfluss, J. and Lauterborn, W., Predicting chaotic time series, *Phys. Rev. A*, **39**, 2146-2152, 1989.
- Isham, V., Statistical aspects of chaos: A review, in *Networks and chaos: statistical and probabilistic aspects*, edited by O. E. Barndorff-Nielsen, J. L. Jensen, and W. S. Kendall, vol. 50 of *Monographs on Statistics and Applied Probability*, Chapman Hall, 1993.
- Karadonis, A. and Pagitsas, M., Comparative study the calculation of the lyapunov spectrum from nonlinear experiment signals, *Phys. Rev. E*, **53**, 5428-5444, 1995.
- Klimas, A. J., Baker, D. N., Roberts, D. A., Fairfield, D. H., and Buchner, J. A., A nonlinear dynamical analogue model of substorms, in *Magnetospheric Substorms*, edited by J. R. Kan, T. A. Potemra, S. Kokubun, and T. Iijima, pp. 449-459, AGU, Washington, D.C., 1991.
- Klimas, A. J., Vassiliadis, D., Baker, D. N., and Roberts, D. A., The organized nonlinear dynamics of the magnetosphere, *Geophys. Res.*, **101**, 13 089-13 113, 1996.
- Klimas, A. J., Vassiliadis, D., and Baker, D. N., Data-derived analogues of the magnetospheric dynamics, *J. Geophys. Res.*, **102**, 26 993-27 009, 1997.
- Kugiumtzis, D., Lingjaerde, O. C., and Christophersen, N., Regularized local linear prediction of chaotic time series, *Physica D*, **112**, 344-360, 1998.
- Lillekjendlie, B., Kugiumtzis, D., and Christophersen, N., Chaotic time series part ii: System identification and prediction, *Modeling, Identification and Control*, **15**, 225-243, 1994.
- McPerron, R. L., Baker, D. N., Bargatze, L. F., Clauer, C. R., and Holzer, R. E., IMF control of geomagnetic activity, *Adv. Space Res.*, **8**, 71, 1988.
- McPherron, R. L., Magnetospheric dynamics, in *Introduction to space physics*, edited by M. G. Kivelson and C. T. Russell, pp. 400-458, Cambridge University Press, 1995.
- Osborne, A. R., Kirwan, A. D., Provenzale, A., and Bergamasco, L., A search for chaotic behavior in large and mesoscale motions in the pacific ocean, *Physica D*, **23**, 75-83, 1986.

- Pavlos, G. P., Kyriakou, G. A., Rigas, A. G., Liatsis, P. I., Trochoutos, P. C., and Tsonis, A. A., Evidence for strange attractor structures in space plasmas, *Ann. Geophys.*, *10*, 309–322, 1992a.
- Pavlos, G. P., Rigas, A. G., Dialelis, D., Sarris, E. T., Karakatsanis, L. P., and Tsonis, A. A., Evidence for chaotic dynamics in outer solar plasma and the earth magnetopause, in *Chaotic Dynamics: Theory and Practice*, edited by A. Bountis, pp. 327–339, Plenum, New York, 1992b.
- Pavlos, G. P., Diamadidis, D., Adamopoulos, A., Rigas, A. G., Daglis, I. A., and Sarris, E. T., Chaos and magnetospheric dynamics, *Nonlin. Proc. Geophys.*, *1*, 124–135, 1994.
- Pavlos, G. P., Athanasiou, M. A., Diamantidis, D., Rigas, A. G., and Sarris, E. T., Comments and new results about the magnetospheric chaos hypothesis, accepted for publication in *Nonlin. Proc. Geophys.*, 1999a.
- Pavlos, G. P., Athanasiu, M., Kugiumtzis, D., Hatzigeorgiu, N., Rigas, A. G., and Sarris, E. T., Nonlinear analysis of magnetospheric data, part I. geometric characteristic of the ae index time series and comparison with nonlinear surrogate data., accepted for publication in *Nonlinear Proc. Geophys.*, 1999b.
- Price, C. P. and Prichard, D. J., The non-linear response of the magnetosphere: 30 october 1978, *Geophys. Res. Lett.*, *20*, 771–774, 1993.
- Price, C. P., Prichard, D., and Bischoff, J. E., Nonlinear input-output analysis of the auroral electrojet index, *J. Geophys. Res.*, *99*, 13 227–13 238, 1994.
- Prichard, D. J., Short comment for magnetospheric chaos, *Nonlinear Proc. Geophys.*, *20*, 771–774, 1994.
- Provenzale, A., Osborne, A. R., Jr., A. D. K., and Bergamasco, L., The study of fluid parcel trajectories in large-scale ocean flows, in *Nonlinear Topics in Ocean Physics*, edited by A. R. Osborns, vol. 64, pp. 367–402, Elsevier, Paris, 1991.
- Robert, D. A., Baker, D. N., Klimas, A. J., and Bargatze, L. F., Indications of low dimensionality in magnetospheric dynamics, *Geophys. Res. Lett.*, *18*, 151–154, 1991.
- Sano, M. and Sawada, Y., *?*, *Phys. Rev. Lett.*, *55*, 1082, 1985.
- Schreiber, T., Constrained randomization of time series data, *Phys. Rev. Lett.*, *80*, 2105–2108, 1998.
- Schreiber, T. and Schmitz, A., Improved surrogate data for nonlinearity test, *Phys. Rev. Lett.*, *77*, 635–638, 1996.
- Shan, H., Hansen, P., Goertz, C. K., and Smith, K. A., Chaotic appearance of the ae index, *Geophys. Res. Lett.*, *18*, 147–150, 1991.
- Shaw, R. Z., Strange attractors, chaotic behavior and information flow, *Z. Naturforsch.*, *36a*, 80–122, 1981.
- Shaw, R. Z., *The dripping faucet as a model dynamical system*, Aerial Press, Santa Cruz, 1984.
- Sugihara, G. and May, R. M., Nonlinear forecasting as a way of distinguishing chaos from measurement error in time series, *Nature*, *344*, 734–741, 1990.
- Takens, F., Detecting strange attractors in turbulence, in *Lectures Notes in Mathematics*, edited by D. A. Rand and L. S. Young, vol. 898, pp. 366–381, Springer, Berlin, 1981.
- Theiler, J., Eubank, S., Longtin, A., Galdikian, B., and Farmer, J. D., Testing for nonlinearity in time series: the method of surrogate data, *Physica D*, *58*, 77–94, 1992a.
- Theiler, J., Galdikian, B., Longtin, A., Eubank, S., and Farmer, J. D., Using surrogate data to detect nonlinearity in time series, in *Nonlinear Modeling and Forecasting*, edited by M. Casdagli and S. Eubank, vol. XII of *SFI studies in the Sciences of Complexity*, pp. 163–168, Addison-Wesley, Reading, Mass., 1992b.
- Tsonis, A. A., *Chaos: From theory to applications*, Plenum Press, New York, 1992.
- Vassiliadis, D., Sharma, A. S., Eastman, T. E., and Papadopoulos, K., Low-dimensional chaos in magnetospheric activity from ae time series, *Geophys. Res. Lett.*, *17*, 1841–1844, 1990.
- Vassiliadis, D., Sharma, A. S., and Papadopoulos, K., Time series analysis of magnetospheric activity using nonlinear dynamical methods, in *Chaotic Dynamics: Theory and Practice*, edited by A. Bountis, Plenum, New York, 1992.
- Weigend, A. S. and Gershenfeld, N. A., *Time Series Prediction: Forecasting the Future and Understanding the Past*, Addison-Wesley Publishing Company, Reading, 1993.
- Wolf, A., Swift, J. B., Swinney, H., and Vastano, J. A., Determining Lyapunov exponents from a time series, *Physica D*, *16*, 285–317, 1985.